Reducing stomatal density in barley improves drought tolerance without impacting on yield

Hughes, Jonathan; Hepworth, Christopher; Dutton, Christian; Dunn, Jessica A.; Hunt, Lee; Stephens, Jennifer

Published in:
Plant Physiology

DOI:
10.1104/pp.16.01844

Publication date:
2017

Reducing Stomatal Density in Barley Improves Drought Tolerance without Impacting on Yield[1][CC-BY]

Jon Hughes[2], Christopher Hepworth[2], Chris Dutton, Jessica A. Dunn, Lee Hunt, Jennifer Stephens, Robbie Waugh, Duncan D. Cameron, and Julie E. Gray*

Department of Molecular Biology and Biotechnology, University of Sheffield, Sheffield S10 2TN, United Kingdom (J.H., C.D., J.A.D., L.H., J.E.G.); Department of Animal and Plant Sciences, University of Sheffield, Sheffield S10 2TN, United Kingdom (C.H., D.D.C.); and The James Hutton Institute, Invergowrie, Dundee AB15 8QH, Scotland (J.S., R.W.)

ORCID IDs: 0000-0002-7866-8567 (C.H.); 0000-0002-4625-2233 (J.A.D.); 0000-0001-6781-0540 (L.H.); 0000-0002-5761-9782 (J.S.); 0000-0003-1045-3065 (R.W.); 0000-0002-5439-6544 (D.D.C.); 0000-0001-9972-5156 (J.E.G.).

The epidermal patterning factor (EPF) family of secreted signaling peptides regulate the frequency of stomatal development in model dicot and basal land plant species. Here, we identify and manipulate the expression of a barley (*Hordeum vulgare*) ortholog and demonstrate that when overexpressed HvEPF1 limits entry to, and progression through, the stomatal development pathway. Despite substantial reductions in leaf gas exchange, barley plants with significantly reduced stomatal density show no reductions in grain yield. In addition, HvEPF1OE barley lines exhibit significantly enhanced water use efficiency, drought tolerance, and soil water conservation properties. Our results demonstrate the potential of manipulating stomatal frequency for the protection and optimization of cereal crop yields under future drier environments.

With the global population set to rise to over 9 billion by 2050 and the predicted instability in global climate patterns, fears over global food security continue to grow (Godfray et al., 2010). Prolonged periods of drought and expanded zones of desertification are expected to become increasingly prevalent as this century progresses (IPCC, 2014). The need to expand agriculture into areas of marginal land, where drought is a severe inhibitor of sustainable agriculture (Fita et al., 2015), continues to increase. Seventy percent of global freshwater is already utilized for irrigation, and rainfed agriculture is now the world's largest consumer of water (Foley et al., 2011). A potential way to both futureproof against climate change and to expand crop production onto water-limited marginal lands would be through improvements to crop drought tolerance and water use efficiency (WUE; the ratio of carbon gained to water lost).

The vast majority of water is lost from crops via transpiration, and reducing this loss provides a potential route toward improving WUE and conserving soil water levels (Hepworth et al., 2015). To this end, much research into the use of antitranspirants was carried out in the 1960s and 1970s (Davenport et al., 1972). However, although effective in improving water status and increasing fruit size, these chemical solutions were never economically viable on an agricultural scale.

The majority of water loss from plants occurs via transpiration through epidermal pores known as stomata, making these cellular structures an attractive target in the battle to prevent water loss. Recently several laboratory studies have demonstrated that it is possible to improve drought tolerance and WUE by reducing the frequency of stomata on leaves; by using genetic manipulation or mutation to reduce stomatal density improved WUE has been achieved across several model dicot species including Arabidopsis (*Arabidopsis thaliana*; Yoo et al., 2010; Franks et al., 2015; Hepworth et al., 2015), poplar (*Populus* spp.; Lawson et al., 2014), and tobacco (*Nicotiana tabacum*; Yu et al., 2008). In addition, the ectopic expression of a putative transcription factor in maize (*Zea mays*) has led to reduced stomatal density and gas exchange in a monocot (Liu et al., 2015).

The manipulation of stomatal density has been facilitated by microscopic studies that characterized the cellular stages of the stomatal lineage and molecular

[1] This work was supported by the BBSRC, EPSRC, the Gatsby Charitable Foundation, and the Grantham Foundation for Sustainable futures.

[2] These authors contributed equally to the article.

* Address correspondence to j.e.gray@sheffield.ac.uk.

The author responsible for distribution of materials integral to the findings presented in this article in accordance with the policy described in the Instructions for Authors (www.plantphysiol.org) is: Julie E. Gray (j.e.gray@sheffield.ac.uk).

J.H. and C.H. performed barley physiological and statistical analyses; C.H. and J.H. performed the confocal microscopy; C.D. performed qPCR; J.H. carried out Arabidopsis experiments; J.A.D. contributed to the stomatal analysis; L.H., J.S., and R.W. performed barley gene cloning and transformation; J.E.G., L.H., and R.W. conceived and supervised the project; C.H. created the figures; and C.H., J.H., and J.E.G. analyzed the data and wrote the article with input from the other authors.

www.plantphysiol.org/cgi/doi/10.1104/pp.16.01844

studies that revealed the developmental mechanisms controlling their progression (Zhao and Sack, 1999; Han and Torii, 2016). The majority of these studies have been carried out using the genetically tractable, model plant species Arabidopsis. During early Arabidopsis leaf development, a subset of epidermal cells known as meristemoid mother cells become primed to enter the stomatal lineage. Each meristemoid mother cell then undergoes an initial asymmetric entry division to produce a meristemoid in addition to a larger daughter cell known as a stomatal lineage ground cell (SLGC). SLGCs either differentiate directly into epidermal pavement cells or undergo further asymmetric divisions to produce secondary meristemoids. Some meristemoids can themselves undergo further asymmetric divisions, each of which reforms a meristemoid and creates an additional SLGC. Each meristemoid eventually differentiates into a guard mother cell, small and rounded in shape, prior to undergoing a symmetric division to form the guard cell pair of the mature stomatal complex. These cell fate transitions and divisions, which ultimately control the number and proportions of stomata and pavement cells in the mature leaf epidermis, are controlled by a subgroup of related basic helix-loop-helix (bHLH) transcription factors; SPCH, MUTE, and FAMA (Ohashi-Ito and Bergmann, 2006; MacAlister et al., 2007; Pillitteri and Torii, 2007). SPCH primarily directs expression of genes controlling meristemoid formation including members of the Cys-rich EPIDERMAL PATTERNING FACTOR (EPF) family of secreted signaling peptides, which in turn activate a pathway that regulates SPCH stability, thus forming a feedback loop that regulates the number of cells entering the stomatal lineage (Adrian et al., 2015; Simmons and Bergmann, 2016). The best characterized negative regulators of stomatal density in this peptide family are EPF1 and EPF2, which are numbered in order of their discovery (Hara et al., 2007, 2009; Hunt and Gray, 2009). Both peptides act extracellularly within the aerial epidermal cell layer to suppress stomatal development through activation of an intracellular MAP kinase signaling pathway (Bergmann et al., 2004; Wang et al., 2007; Lampard et al., 2008). Although their functions somewhat overlap, EPF2 acts earliest in stomatal development to restrict entry of cells into the stomatal lineage, while EPF1 acts later to orient subsequent divisions of meristemoid cells and enforce stomatal spacing through the "one-cell-spacing" rule via the inhibition of MUTE expression (Hara et al., 2007; Qi et al., 2017). Manipulation of the expression levels of these peptides in Arabidopsis has led to significant improvements in drought tolerance and WUE in experiments conducted in controlled-environment plant growth rooms (Doheny-Adams et al., 2012; Hepworth et al., 2015).

In contrast to the Arabidopsis model system, our knowledge of stomatal development in crops is relatively limited (Raissig et al., 2016). Although the grasses include many of our major global crops, our molecular understanding of their transpirational control mechanisms remains extremely limited. It is known from microscopic observations that grass stomata are formed by a single asymmetric cell division that forms a stomatal precursor cell (a guard mother cell) and an epidermal pavement cell (Stebbins and Jain, 1960). There are no further asymmetric divisions of the stomatal lineage cells analogous to the repeated possible divisions that meristemoids undergo in Arabidopsis (Serna, 2011). The mature grass stomatal complex is formed by division of two neighboring cells that give rise to flanking subsidiary cells, and a symmetric division of the guard mother that produces two dumbbell-shaped guard cells rather than the characteristically kidney-shaped guard cells of most dicots (Hetherington and Woodward, 2003; Serna,

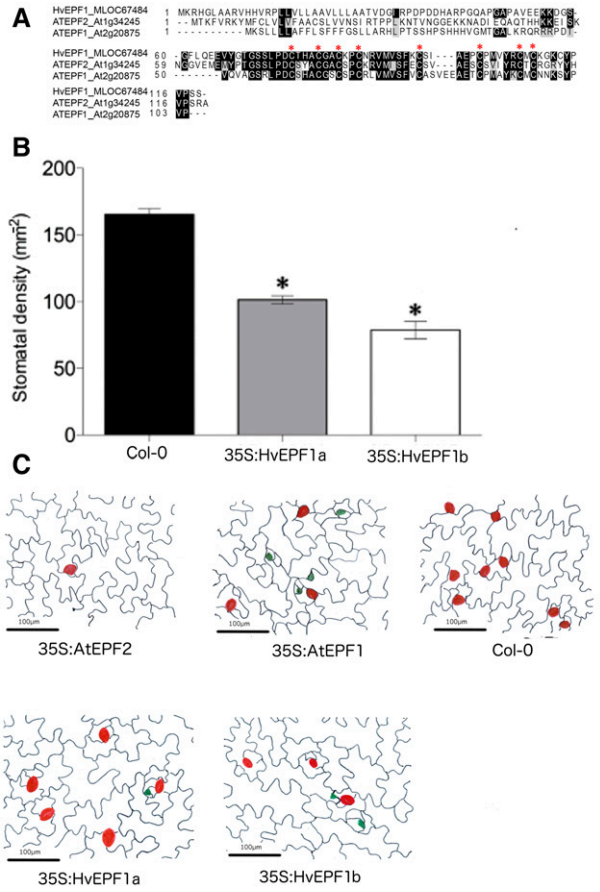

Figure 1. HvEPF1 shares sequence similarity with Arabidopsis EPF1 and EPF2 and can restrict Arabidopsis stomatal development. A, Alignment of the putative HvEPF1 mature signaling peptide with members of the Arabidopsis EPF family of signaling peptides. Conserved Cys residues are highlighted. Amino acid sequences for the mature peptide region were aligned using Multalin and displayed using Boxshade. B, Overexpression of *HvEPF1* under the control of the *CaMV35S* promoter in Arabidopsis leads to a significant decrease in stomatal density. C, Epidermal tracings from Arabidopsis cotyledons overexpressing *EPF1*, *EPF2*, and *HvEPF1* alongside the background control Col-0. Red dots mark location of stomata while green dots mark location of arrested meristemoids. $n = 5$ plants, asterisks indicate $P < 0.05$ (Dunnett's test after one-way ANOVA). Error bars represent SE.

2011). In contrast to dicots, all grass stomatal development initiates at the leaf base. The patterning of stomata within the leaf epidermis also differs in grasses, with stomata forming in straight files parallel to the leaf vein as opposed to the "scattered" distribution seen in Arabidopsis (Stebbins and Khush, 1961; Geisler and Sack, 2002; Serna, 2011)

Despite these differences in stomatal shape and patterning, it appears that the molecular control of stomatal development has similarities across a wide range of plant species. Functional orthologs of genes encoding for bHLH transcription factors involved in Arabidopsis stomatal development have been identified in grasses including rice (*Oryza sativa*), maize (Liu et al., 2009), and brachypodium (Raissig et al., 2016) and recently in the early diverging nonvascular mosses (Chater et al., 2016). EPF orthologs are encoded across a range of plant genomes and have recently been shown to effectively regulate moss stomatal patterning (Caine et al., 2016). However, currently it is still not known whether EPFs function in controlling stomatal development in grasses. With the sequencing of the barley genome in 2012, we were able to identify a putative EPF ortholog (*HvEPF*1, MLOC_67484) that is expressed at low levels during development of aerial tissues (International Barley Genome Sequencing Consortium, 2012). Here, we characterize the function of an epidermal patterning factor in grasses. We report the ectopic overexpression of *HvEPF1* and the production of transgenic barley lines exhibiting altered stomatal development. Furthermore, our generation of barley lines with reduced stomatal density has provided us with the necessary tools to determine the effect of reduced stomatal density on transpiration, drought tolerance, WUE, and yield in a cereal crop.

RESULTS

Eleven genes encoding putative EPF-like secreted peptides were identified in the barley genome sequence (International Barley Genome Sequencing Consortium, 2012; Supplemental Fig. S1). MLOC67484, which we refer to here as *HvEPF1*, encodes a peptide with extensive similarity to Arabidopsis epidermal patterning factors and contains the six conserved Cys residues (Fig. 1A) that are characteristic of Arabidopsis epidermal patterning factors (Ohki et al., 2011; Lau and Bergmann, 2012). Phylogenetic analysis of the encoded mature peptide sequence indicated that within the Arabidopsis EPF family, HvEPF1 is most closely related to the known inhibitors of stomatal development EPF1 and EPF2, which each contain two additional Cys residues (Supplemental Fig. S1). To confirm that this barley peptide gene could function in stomatal regulation, *HvEPF1* was ectopically overexpressed in Arabidopsis under the control of the *CaMV35S* promoter. Analysis of cellular patterning on the epidermis of Arabidopsis plants overexpressing *HvEPF1* confirmed that stomatal development had been disrupted, a

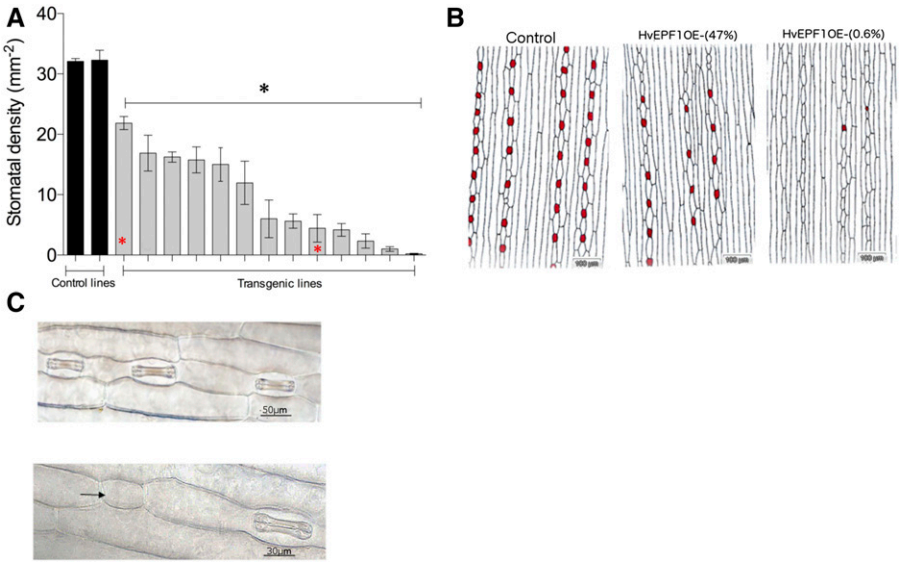

Figure 2. Overexpression of HvEPF1 in barley arrests stomatal development and reduces stomatal density. A, The abaxial stomatal density of barley plants transformed to ectopically overexpress *HvEPF1* (gray bars) compared to control lines transformed with the empty vector (black bars). All T1 generation *HvEPF1* overexpressing lines demonstrated a significant reduction in stomatal density in comparison to both control lines. Lines chosen for further phenotyping in T2 generations are indicated (red asterisks). B, Traced abaxial epidermal impressions of T1 generation control, *HvEPF1OE*- (47%), and *HvEPF1OE*- (0.6%) lines illustrating the reduction in stomatal density. Red dots denote positions of stomatal complexes. C, Abaxial epidermal micrographs of *HvEPF1OE* plants. Black arrow indicates arrested stomatal precursor cell. $n = 4$ to 8 plants. Asterisks indicated significance to at least $P < 0.05$ versus control lines (Dunnett's test after one-way ANOVA. Error bars represent SE.

phenotype similar to that observed on overexpression of Arabidopsis *EPF1*, namely, a significant decrease in leaf stomatal density (Fig. 1B) and an increased number of arrested meristemoids (Fig. 1C; Hara et al., 2007, 2009; Hunt and Gray, 2009).

Next, barley plants ectopically overexpressing the epidermal patterning factor HvEPF1 under the control of a ubiquitin gene promoter were produced. Stomatal density was assessed from 13 transgenic lines of *HvEPF1OE* in the T1 generation under growth room conditions. The first leaves of seedling plants had stomatal densities ranging from ~70% down to <1% of that of control plants (transformed with the empty vector; Fig. 2A). Two lines were selected for further phenotyping: *HvEPF1OE* (47%) and *HvEPF1OE* (0.6%), which displayed ~47% and 0.6% of the stomatal density of controls, respectively. Significantly reduced leaf stomatal density was observed in abaxial epidermal impressions (Fig. 2B), and unusually large patches of epidermis with an absence of stomates were seen in the leaves of HvEPF1OE (0.6%). Furthermore, arrested stomatal precursor cells, frequently observed in the

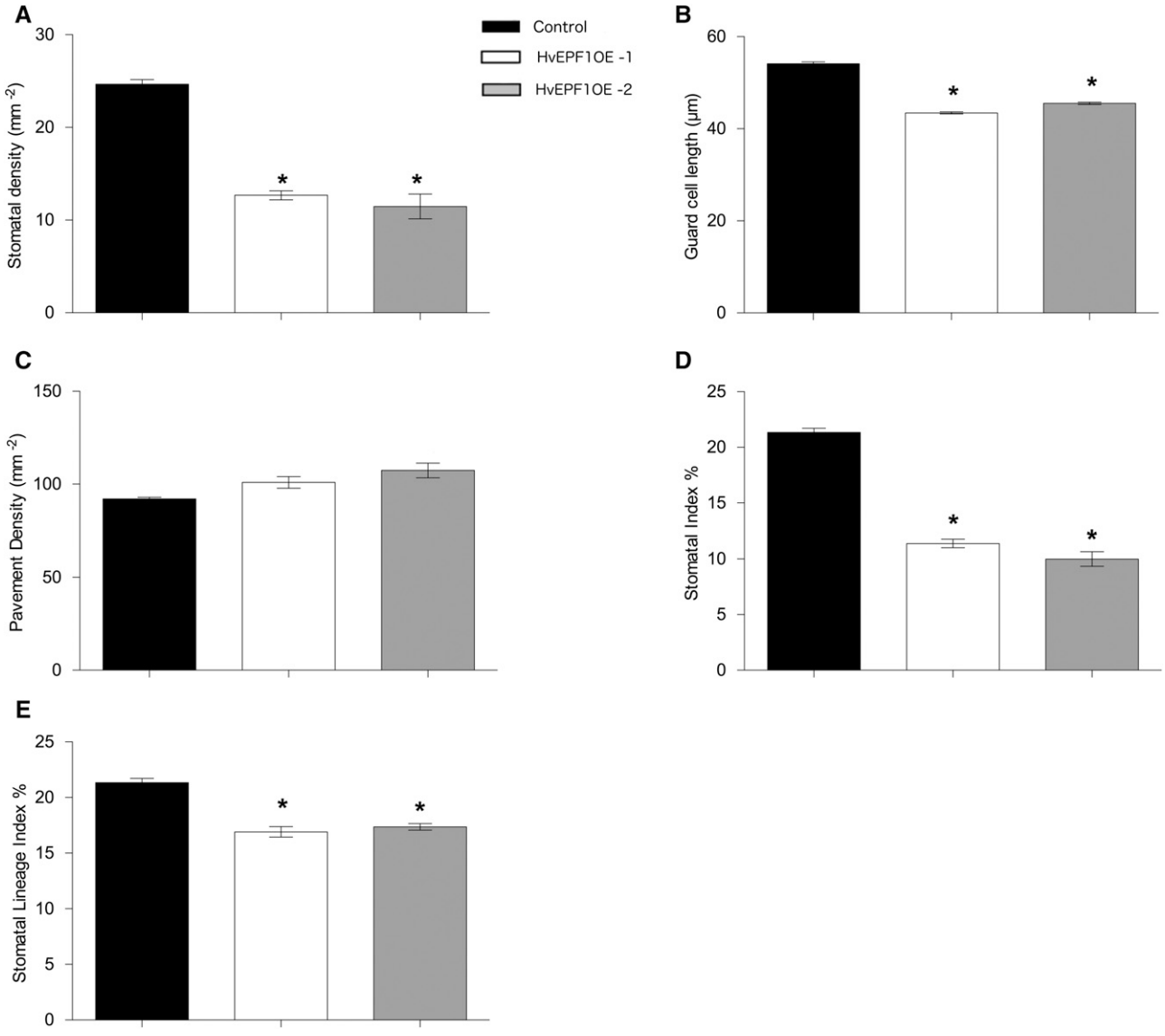

Figure 3. Stomatal characteristics of barley plants overexpressing *HvEPF1*. A, Abaxial stomatal densities of *HvEPF1* overexpressing T2 barley lines harboring a single copy of the transgene are significantly decreased. *HvEPF1OE*-1 (white bars) and *HvEPF1OE*-2 (gray bars) compared to control lines (black bars). B, Guard cell length is significantly decreased in both *HvEPF1OE* lines. C, Pavement cell density is similar to that of the control in both *HvEPF1OE* lines. D, Stomatal index is significantly decreased in both *HvEPF1OE* lines. E, Stomatal lineage index (the ratio of stomata and arrested stomatal precursor cells to the total number of epidermal cells) is significantly decreased in both *HvEPF1OE* lines. $n = 5$ plants, asterisks indicate $P < 0.05$ (Dunnett's test after one-way ANOVA). Error bars represent SE.

mature, fully expanded epidermis, were extremely rare in controls (Fig. 2C, black arrow).

For more detailed physiological analysis, homozygous barley lines harboring a single copy of the transgene (Supplemental Table S1) were isolated (referred to as *HvEPF1OE*-1 and *HvEPF1OE*-2 and indicated by the left and right red asterisks in Figure 2A, respectively). T2 generation plants were grown under controlled chamber conditions, and the abaxial stomatal density of the second true leaf was significantly reduced by ~52% and 56% of controls for *HvEPFOE*-1 and *HvEPFOE*-2, respectively (Fig. 3A). In addition, the stomates that formed were smaller; guard cell length was significantly reduced in both *HvEPF1OE* lines (Fig. 3B). However, we observed no significant increase in epidermal pavement cell density (Fig. 3C). These differences in cell densities combined to produce large reductions in stomatal index (stomatal density as a percentage of all cells on the epidermis). The stomatal index of *HvEPF1OE* plants was reduced to ~50% of control values (Fig. 3D). Again, we observed a significant increase in the number of arrested stomatal precursor cells in *HvEPF1OE* barley leaves (as shown in Fig. 2). To calculate whether the number of arrested stomatal precursor cells could entirely account for the observed reductions in stomatal density, we calculated the stomatal lineage cell index (the percentage of stomata and arrested stomatal lineage cells compared to all cells on the epidermis). This indicated that if all arrested stomatal precursor cells were to have progressed normally to produce stomata, there would still be a significant reduction in stomatal index, suggesting that both the priming of cells to enter the stomatal lineage and the progression of cells through the stomatal lineage are compromised by HvEPF1 overexpression (Fig. 3E).

Having shown that HvEPF1 can effectively regulate the frequency of stomatal development, we next explored whether any other aspects of *HvEPF1OE* leaves were affected. In particular, we investigated the internal structure of leaves. Stacked confocal images were produced to visualize *HvEPF1OE* substomatal cavities. This revealed similar internal cellular structures, and mature *HvEPF1OE* stomatal complexes had guard cells positioned normally above substomatal cavities as in controls (Fig. 4A, yellow asterisks). However, on the same images, a lack of cavity formation was observed under the arrested stomatal precursor cells in both *HvEPF1OE*-1 and *HvEPF1OE*-2 lines (Fig. 4B, white asterisks).

To more fully investigate the effect of reduced stomatal density on drought tolerance, T2 generation plants were grown in a greenhouse with natural and supplemental lighting and temperature control. Five-week-old *HvEPF1OE*-1, *HvEPF1OE*-2, and control plants were subjected to a terminal drought experiment alongside a parallel set of plants that were kept well watered (maintained at 60% maximum soil water content). Pots were weighed at the same time each day and this was used to calculate soil water loss. The results of

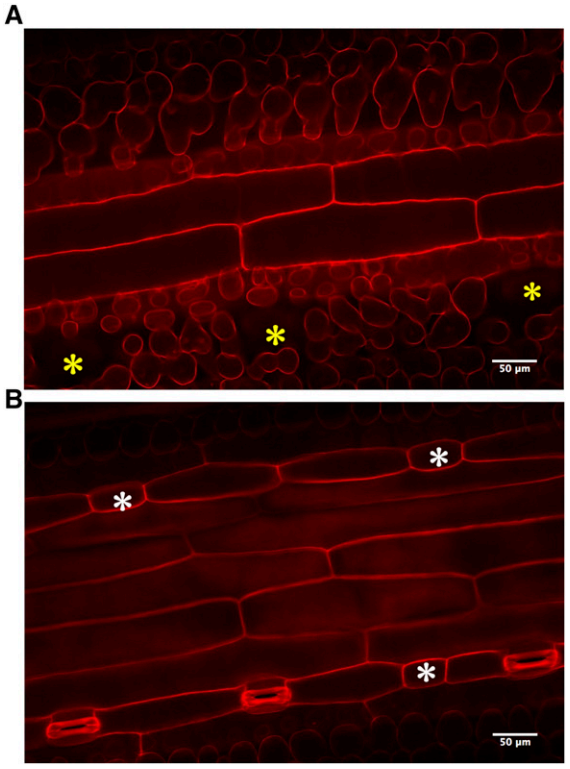

Figure 4. Cellular structure of *HvEPF1OE* stomatal complexes. A, Representative propidium iodide-stained confocal image of a Z-plane below the *HvEPF1OE*-1 abaxial epidermal surface. Yellow asterisks mark the location of the substomatal cavity under mature guard cells. B, Higher Z-plane image of the same field of view as A to reveal position of stomata. White asterisks mark the location of arrested stomatal precursors and the lack of underlying substomatal cavities in A.

this experiment revealed that both transformed barley lines lost water much more slowly and exhibited significantly greater soil water conservation in their pots from day 2 until day 14 under water-withheld conditions (Fig. 5A). Chlorophyll fluorescence measurements were used to measure any reductions in PSII efficiency, an indicator of plant stress. The light-adapted quantum yield of PSII (Φ_{PSII}) was measured daily for both well-watered and water-withheld plants throughout the terminal drought experiment. There were no differences between the Φ_{PSII} of *HvEPF1OE* and control plants at the start of the experiment or between genotypes under well-watered conditions, indicating that the reduced stomatal density of the *HvEPF1OE* leaves was not restricting PSII efficiency. Remarkably, however, the *HvEPF1OE* plants that had water withheld displayed significantly enhanced rates of Φ_{PSII} versus water-withheld controls from day 10 until day 14; both *HvEPF1OE*-1 and *HvEPF1OE*-2 plants maintained their PSII efficiency for ~4 d longer than controls under severe drought conditions. On day 6 of terminal drought, leaf samples were taken for leaf relative water content (RWC) estimation. This result indicated no significant difference in leaf RWC between controls and

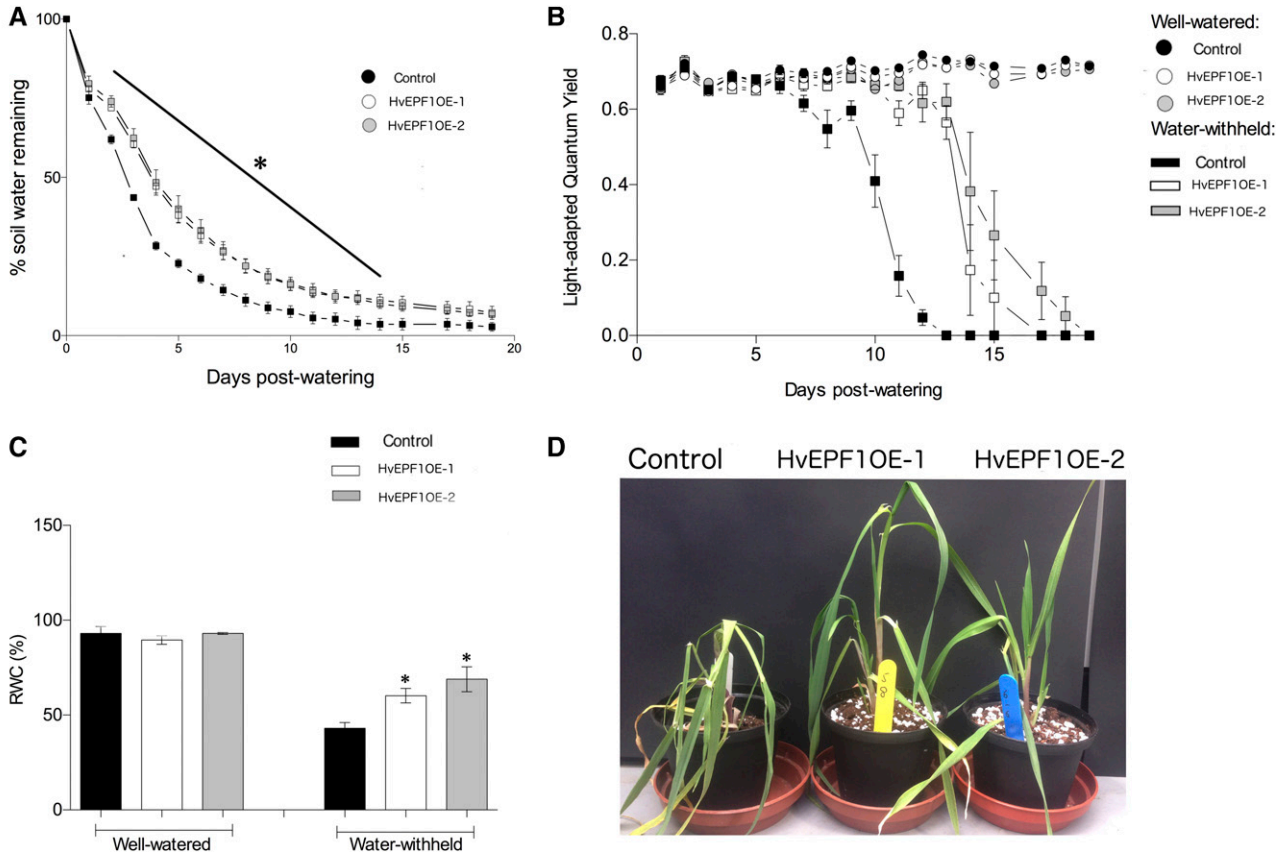

Figure 5. Reducing barley stomatal density enhances drought tolerance though conserving soil and plant water content. A, Five-week-old *Hv*EPF1OE-1 and *Hv*EPF1OE-2 barley plants maintain significantly higher soil water content in comparison to control plants when water is withheld from days 2 to 14. B, Both *Hv*EPF1OE-1 and *Hv*EPF1OE-2 lines show significantly higher ΦPSII from 10 to 14 d after water was withheld (square symbols; plants from same experiment as A. There were no significant differences between ΦPSII of well-watered plants (circular symbols). C, RWC of barley leaves from *Hv*EPF1OE lines was significantly higher than controls after 6 d without watering. There were no differences in RWC between well-watered plants. D, Photograph of representative plants to illustrate enhanced turgor maintenance in *Hv*EPF1OE-1 and *Hv*EPF1OE-2 on day 6 of water-withheld conditions. $n = 5$ plants, asterisk indicates significance to at least $P < 0.05$ (Dunnett's tests after one-way ANOVA for each watering group). Error bars represent SE.

HvEPF1OE plants under well-watered conditions. However, under water-withheld conditions, both *HvEPF1OE* lines displayed significantly higher levels of leaf RWC versus controls (Fig. 5C), indicating an enhanced ability to retain water in their leaves under drought conditions. In addition, the *HvEPF1OE* plants were less susceptible to wilting and appeared visibly more drought tolerant on day 6 of water-withheld conditions (Fig. 5D).

In a separate greenhouse experiment, we investigated whether the reduced stomatal density of *HvEPF1OE* barley plants could confer any advantage to growth under conditions of limited water availability (rather than on complete withholding of water as above). *HvEPF1OE*-1, *HvEPF1OE*-2, and controls plants were grown under well-watered (60% soil water content) and water-restricted (25% soil water content) conditions in parallel under controlled greenhouse conditions. This water-restricted regime was severe enough to attenuate the growth rate of the barley plants but not severe enough to cause visible signs of wilting (Supplemental Fig. S2). Stomatal density and steady-state gas exchange measurements were taken from the sixth fully expanded leaf of the primary tiller of mature plants. This revealed that stomatal density and photosynthetic assimilation were significantly reduced in comparison to controls in both *HvEPF1OE* lines under well-watered conditions. On these leaves, the stomatal density of HvEPF1 OE-1/2 was 24% and 12% of control values, respectively. There was a significant decrease in assimilation in both lines under well-watered conditions but no significant differences in assimilation between *HvEPF1OE* or control plants that had been grown under water restriction (Fig. 6A). In addition, there was a significant reduction in stomatal conductance (*gs*) between *HvEPF1OE* and control plants within the well-watered treatment group and a reduction in the *gs* of all plants within the water-restricted treatment (Fig. 6B). As a result of the large

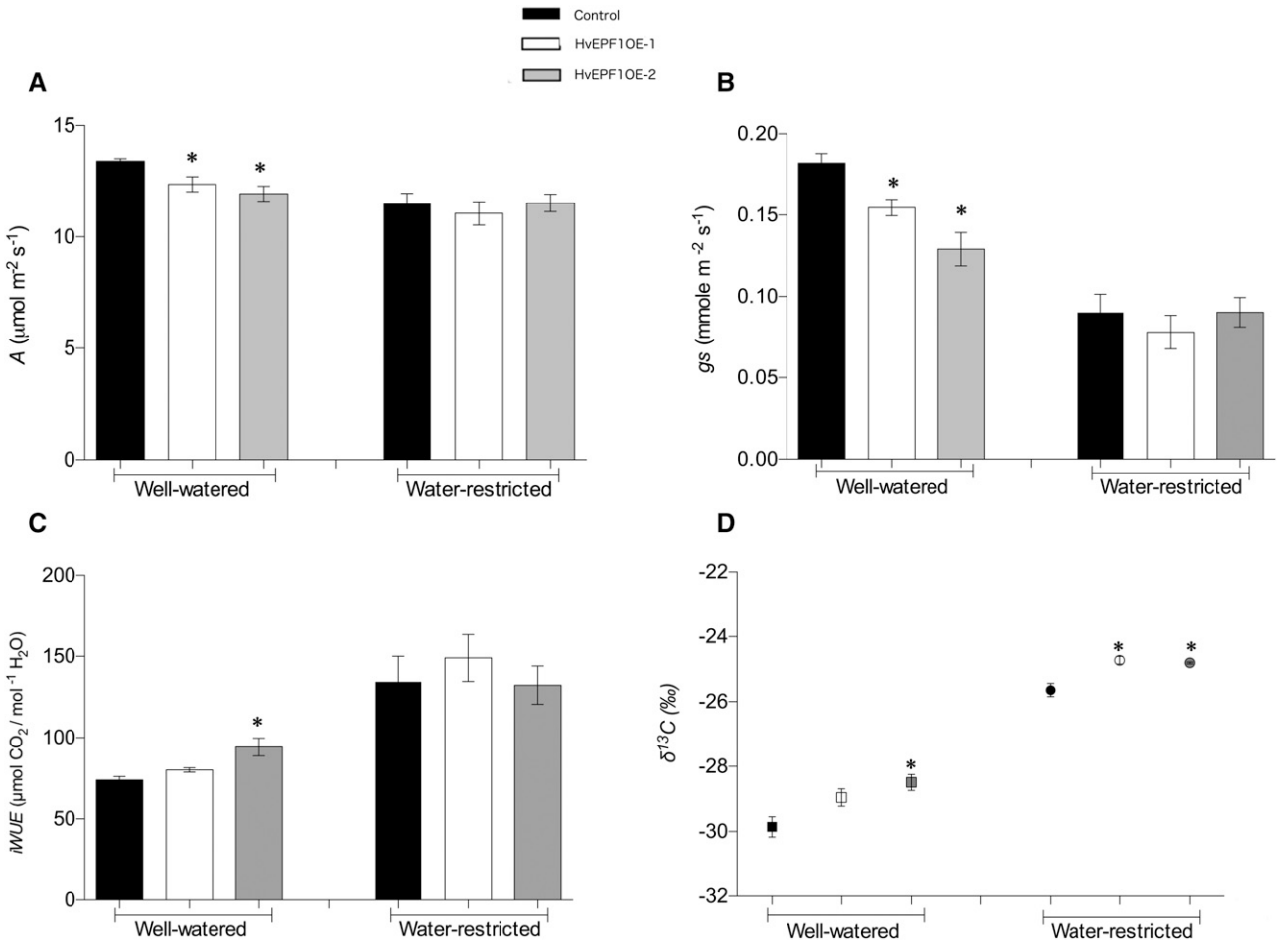

Figure 6. Reducing barley stomatal density lowers *gs* and enhances WUE. A, Under well-watered conditions, a significant decrease in rate of carbon assimilation was observed in both *HvEPF1OE* lines. Under water-restricted conditions, there was no difference in assimilation. B, *gs* was significant decreased in *HvEPF1OE* lines grown under well-watered conditions in comparison to controls. Under water-restricted conditions, there was no difference in *gs*. C, Under well-watered conditions, a significant improvement in iWUE was observed in the *HvEPF1OE*-2 line when compared to control plants. Under water-restricted conditions, there was no difference in iWUE. D, Carbon isotope discrimination revealed a significant improvement in WUE of the *HvEPF1OE*-2 barley line under well-watered conditions. Under water-restricted conditions, both *HvEPF1OE* lines displayed significantly improved WUE in comparison to controls. $n = 5$ plants, asterisk indicates significance to at least $P < 0.05$ (Dunnett's tests after one-way ANOVA for each watering group). Error bars represent SE.

reductions in *gs* and relatively small reductions in assimilation, intrinsic WUE (iWUE, the value of assimilation divided by *gs*) was calculated to be significantly increased in the *HvEPF1OE*-2 line under well-watered conditions. There was no increase in iWUE observed in either *HvEPF1OE* line under water-restricted conditions (Fig. 6C). After 11 weeks of drought, WUE across the photosynthetic lifetime of the barley flag leaves was then assessed by delta-carbon isotope analysis. This revealed that, under water restriction, both *HvEPF1OE* lines displayed lower levels of ^{13}C discrimination and thus a greater level of WUE. In agreement with the gas exchange results, only *HvEPF1OE*-2 plants (which had more severely reduced stomatal density) displayed increased WUE under well-watered conditions (Fig. 6D).

Further gas exchange measurements were carried out on the flag leaf to investigate whether photosynthetic biochemistry could have been altered by overexpression of *HvEPFL1*. In line with our previous Arabidopsis-based studies (Franks et al., 2015), we observed no differences in the maximum velocity of Rubisco for carboxylation or the potential rate of electron transport under saturating light. Our calculations indicate that any improvements in WUE are due to increased limitation to stomatal gas exchange, rather than altered photosynthetic biochemistry.

Finally, to assess the impact of reduced stomatal density on barley yield and biomass, plants were left to grow under the well-watered and water-restricted regimes described above until plant peduncles had lost color. At this point, plants were allowed to dry and

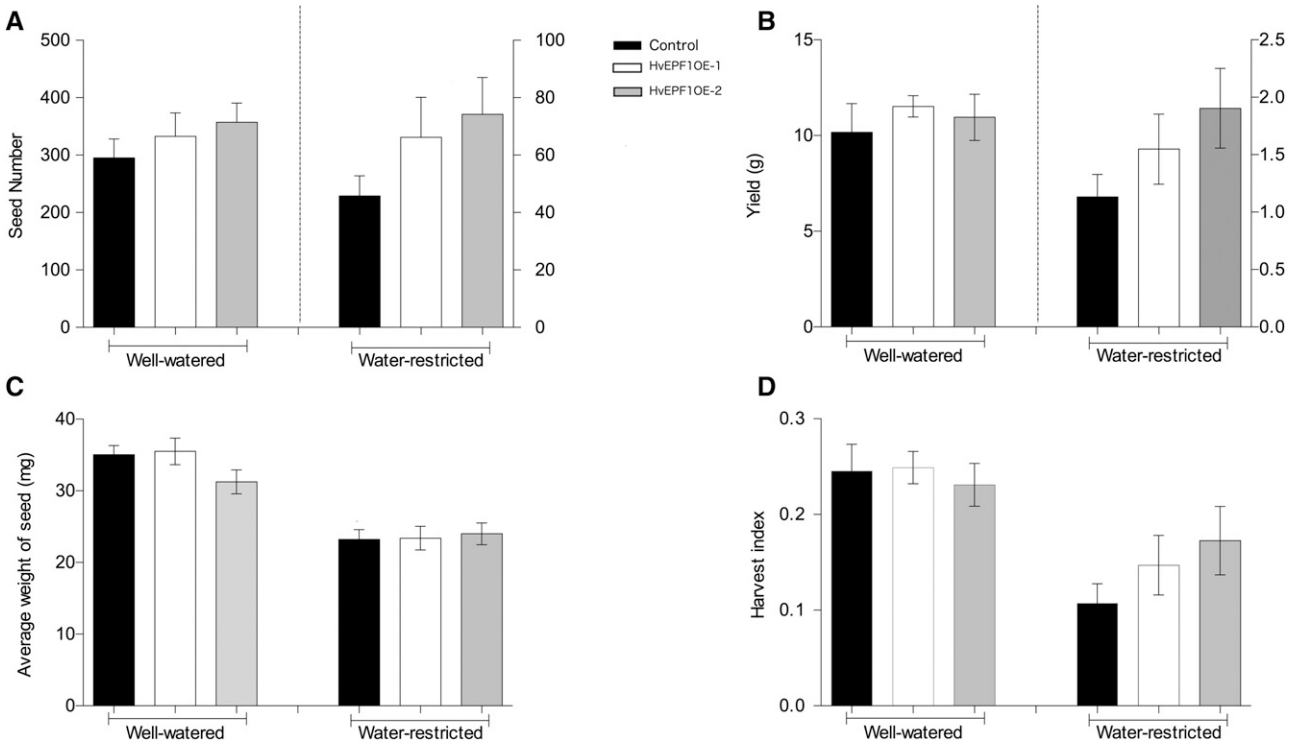

Figure 7. Reducing stomatal density in barley had no deleterious effect on yield. No significant differences in seed number, total weight of seed per plant (B), average weight of individual seeds (C), or harvest index (D; the ratio of yield to total shoot biomass) were observed between *HvEPF1OE*-1, *HvEPF1OE*-2, and control plants under either watering condition. $n = 5$ plants. Error bars represent SE.

were then harvested. Analysis of the grain yield suggested that a reduction in stomatal density did not have a deleterious effect on seed number, seed weight, the average weight of seed, or the harvest index (the ratio of above ground biomass to seed weight) under either watering condition (Fig. 7, A–D). In addition, no differences in plant height or aboveground biomass were found between any of the barley lines under either watering regime (Supplemental Figs. S3 and S4).

DISCUSSION

Grasses are an economically important plant group, with the cereal grasses being of critical importance for both food and energy production. Considering future predicted climate scenarios, the creation of drought-tolerant cereals is a priority area for both crop improvement and scientific research.

The bHLH transcription factors and epidermal patterning factors that were first discovered to be regulators of stomatal development in Arabidopsis have been conserved from basal land plants through to angiosperms, including the grasses, and have been suggested as potential targets for crop improvement (Peterson et al., 2010; Ran et al., 2013; Caine et al., 2016; Raissig et al., 2016). Here, we report the characterization of a functional barley EPF ortholog, named HvEPF1, which acts in a similar way to the Arabidopsis EPF1 and EPF2 signaling peptides to limit entry to and progression through the stomatal cell lineage. Our overexpression of the barley *HvEPF1* transcript in Arabidopsis led to a significant reduction in stomatal density, indicating a level of conservation in peptide function between monocots and dicots. The overexpression of HvEPF1 in barley led to severe reductions in both stomatal formation and the entry of epidermal cells into the stomatal lineage, adding weight to this conclusion.

The frequent presence of arrested stomatal precursor cells on the epidermis of both Arabidopsis and barley *HvEPF1OE* plants (Figs. 1C and 2B) suggests that the mode of action of HvEPF1 is most similar to that of Arabidopsis EPF1, which generates a similar epidermal phenotype when overexpressed (Hara et al., 2007, 2009). That is, stomatal precursors enter the developmental lineage but become arrested before the final symmetric cell division and maturation of the stomatal complex. These *HvEPF1OE* oval-shaped arrested cells appear to halt their development at a meristemoid-like or early guard mother cell stage prior to transition into mature guard mother cells. Thus, in addition to entry to the stomatal lineage, the transition to a mature guard mother cell that is competent to divide and form a pair of guard cells appears to be regulated by HvEPF1. In Arabidopsis, this cellular transition step is under the control of the transcription factor MUTE (Fig. 8) whose

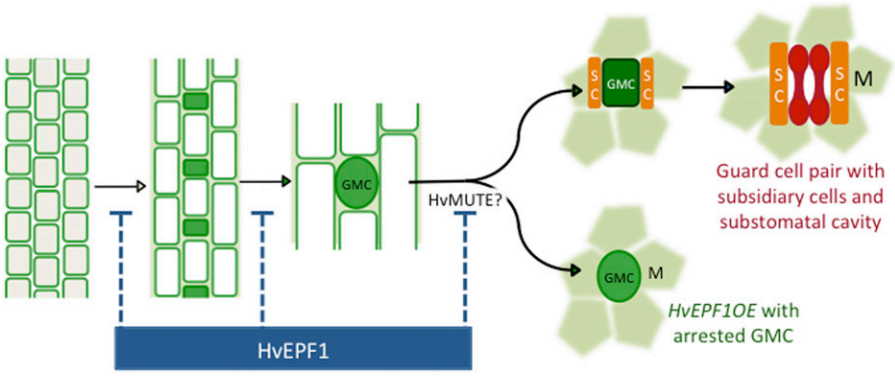

Figure 8. HvEPF1 acts to prevent cells entering the stomatal lineage, guard mother cell maturation, and substomatal cavity and subsidiary cell formation. Schematic to illustrate the putative mode of action of HvEPF1 in barley stomatal development. Left to right: Undifferentiated epidermal cells at the base of leaves are formed in cellular files. Cells in some files gain the capacity to divide asymmetrically to create small stomatal precursor cells shown here as immature guard mother cells (GMC, green). A developmental step, potentially under the control of the transcription factor MUTE, stimulates guard mother cell maturation (dark green) and division of adjacent epidermal cells to form subsidiary cells (SC, orange). Mature GMCs then divide symmetrically to form pairs of dumbbell-shaped guard cells (red). In the underlying mesophyll layer (M, green shaded regions), a substomatal cavity forms during either the mature GMC or guard cell stage, although the exact developmental staging of this is process is unknown. In the *HvEPF1* overexpressing plants, HvEPF1 prevents GMC maturation, perhaps through the suppression of MUTE activity, resulting in arrested GMCs that are unable to differentiate into mature stomatal complexes complete with subsidiary cells, guard cells, and substomatal cavities. Drawn with reference to *Brachypodium* development in Raissig et al. (2016).

activity promotes expression of the receptor-like kinase ERECTA-LIKE1, which in turn mediates EPF1 signaling and the subsequent autocrine inhibition of MUTE (Qi et al., 2017). Barley MUTE may be regulated by HvEPF1 by a similar autocrine pathway and/or by phosphorylation as grass *MUTE* genes (unlike Arabidopsis *MUTE*) encode potential MAP kinase phosphorylation sites (Liu et al., 2009). Recent work in the monocot *Brachypodium* has revealed MUTE is also involved in the formation of subsidiary cells (Raissig et al., 2017). In *HvEPF1OE* plants, stomatal precursors arrest prior to the establishment of subsidiary cells, suggesting the overexpression of HvEPF1 may act to inhibit the expression of MUTE.

Despite their importance, we know remarkably little about the sequence of events leading to the production of the air-filled spaces that underlie stomata. In conjunction with the stomatal pores, these substomatal cavities facilitate high levels of gas exchange into plant photosynthetic mesophyll cells and mediate leaf water loss via transpiration. Using confocal microscopy, we could see no evidence for the separation of mesophyll cells below arrested stomatal precursor cells in HvEPF1OE leaves. Our observations begin to throw light on the developmental sequence leading to cavity formation. The arrested stomatal precursor cells in *HvEPF1OE* do not form substomatal cavities, suggesting that these cavities form following either guard mother cell maturation, like the subsidiary cells of the stomatal complex, or after guard cell pair formation. Alternatively, the formation of a substomatal cavity may be required for guard mother cell maturation.

There is much evidence to support a negative correlation between stomatal density and stomatal size across a range of species and Arabidopsis stomatal mutants, that is, those plants with relatively low stomatal density tend to produce larger stomates (Miskin and Rasmusson, 1970; Franks and Beerling, 2009; Doheny-Adams et al., 2012). Interestingly, the overexpression of HvEPF1 did not conform to this trend and led to barley plants with smaller, shorter guard cells. Thus, if the EPF signaling pathway directly regulates stomatal size in dicot species (and this remains to be demonstrated), it appears to act in the opposite manner in grass stomatal size determination.

Through the ectopic overexpression of HvEPF1 we have created barley transformants with a range of reductions in stomatal density. Although barley plants with substantially reduced numbers of stomata showed some attenuation of photosynthetic rates when well watered, they exhibited strong drought avoidance and drought tolerance traits when water was withheld. They had lower levels of water loss via transpiration, they were able to maintain higher levels of soil water content, and they delayed the onset of photosynthetic stress responses for several days longer than controls. Remarkably, when grown under water-limiting conditions (25% soil pot water content), two barley lines with reductions in stomatal density demonstrated significant improvements in WUE without any deleterious effects on either plant growth or seed yield (biomass, seed weight, or seed number). Indeed, it would be interesting to determine whether both WUE and yield may be further optimized in reduced stomatal density lines under less severe watering regimes or through less drastic reductions in stomatal density.

HvEPF1OE-2 plants (which had the lowest stomatal density in this experiment) also displayed significantly

enhanced levels of drought tolerance and WUE under well-watered conditions, without accompanying decreases in either grain yield or plant biomass. The increased iWUE observed in these experiments was a result of a relatively moderate drop in assimilation compared to a larger decrease in *gs*, suggesting that assimilation was not limited by internal CO_2 concentration under the growth conditions of our experiment (Yoo et al., 2009). This may also be a factor in explaining why reductions in stomatal density did not impact on the yield of *HvEPF1OE* plants. Further explanations include significantly reduced rates of *gs* and thus water loss in *HvEPF1OE* plants allowing for more resources to be allocated to the generation of seed and aboveground biomass, at the potential cost to root development, as described previously in Arabidopsis EPF-overexpressing plants (Hepworth et al., 2016), or increased soil water content leading to improved nutrient uptake and *gs* under water limitation (Van Vuuren et al., 1997; Hepworth et al., 2015). Thus, although not tested in this study, reducing stomatal density may also enhance resource allocation or nutrient uptake capacity under water restriction.

To conclude, this study describes the function and physiological effect of overexpressing a native epidermal patterning factor in a grass species. The manipulation of *HvEPF1* expression levels has improved our understanding of stomatal developmental mechanisms in grasses and has generated a range of barley plants displaying significantly reduced stomatal density. These barley plants exhibit substantially improved drought tolerance and WUE without reductions in grain yield. This discovery adds strength to the proposition that stomatal development represents an attractive target for breeders when attempting to future-proof crops.

MATERIALS AND METHODS

Vector Construction

HvEPF1 genomic gene was PCR amplified from barley (*Hordeum vulgare*) cultivar Golden Promise DNA using primers in Supplemental Table S1. The HVEPF1 gene is annotated as MLOC67484 at Ensembl Plants but is incorrectly translated in this prediction. We used FGENESH to generate an alternative translation, which includes a putative signal sequence at the N terminus. The PCR product was recombined pENTR/D/TOP0 then by LR recombination into pCTAPi (Rohila et al., 2004) transformation vector under the control of the CaMV35S promoter, and introduced into Arabidopsis (*Arabidopsis thaliana*) Col-0 background by floral dip (Clough and Bent, 1998). Transformation and expression of the transgene were confirmed by PCR and RT-PCR using the primers in Supplemental Table S2.

For barley transformation, the *HvEPF1* genomic gene was introduced by LR recombination into pBRACT214 gateway vector under the control of the maize (*Zea mays*) ubiquitin promoter, adjacent to a hygromycin resistance gene under the control of a CaMV35S promoter (Supplemental Fig. S4). Barley transformations were carried out in background Golden Promise using the method described by (Harwood et al., 2009). Plants harboring just the hygromycin resistance cassette were regenerated alongside to produce empty-vector control plants. Potentially transformed plants were regenerated on selective medium and T0 individuals genotyped to confirm gene insertion by PCR. Gene copy number was estimated byIDna Genetics Ltd (www.idnagenetics.com) using a PCR-based method. HvEPF1 overexpression was confirmed by RT-qPCR of T2 generation plants (Supplemental Fig. S6). Total RNA was extracted from 10-d-old seedlings using Spectrum plant total RNA kit (Sigma-Aldrich) and reverse transcribed using Maxima H Minus Reverse Transcriptase cDNA synthesis kit (Thermo Scientific). RT-qPCR was performed using a Rotor-Gene SYBR Green PCR kit (Qiagen) with tubulin and GADPH used as housekeeping reference genes, and primers outlined in the supplementary supporting information (Supplemental Table S2). Three plants of each transformed line were amplified to confirm overexpression of the *HvEPF1* gene. Fold induction values of gene expression were normalized to average $2^{\Delta Ct}$ values relative to empty-vector control samples.

Plant Growth Conditions

For plant growth, seeds were surfaced sterilized in 50% (v/v) ethanol/bleach before being placed onto water-saturated filter paper and placed into sealed petri dishes in the appropriate growth chamber. Arabidopsis plants were grown in a controlled growth chamber (Conviron model MTPS120) at 22°C/16°C, 9 h light, 150 to 200 μmol m^{-2} s^{-1}, 15 h dark, ambient [CO_2], and 60% humidity. Arabidopsis plants were kept well watered throughout. Barley plants were grown in a MTPS120 growth chamber at 21°C/15°C, 11 h light at 300 μmol m^{-2} s^{-1}, 13 h dark, ambient [CO_2], and 60% humidity. For plants grown under greenhouse conditions (Figs. 5 and 6), temperature was set at 20°C/16°C, 12 h light, and ambient humidity, and supplementary lighting ensured a minimum of 200 μmol m^{-2} s^{-1} at bench level.

At 5 d postgermination, individual barley seedlings were placed into 13-cm-diameter pots containing homogenized M3 compost/perlite (4:1) with the addition of Osmocote. For initial phenotyping and leaf developmental characterization (Figs. 2–4), plants were kept well watered. For the water-restricted experiment (Figs. 6 and 7), plants were maintained at either 60% (well watered) or 25% (water restricted) of soil saturation by the daily weighing of pots.

Microscopy and Cell Counts

For both Arabidopsis and barley, stomatal and epidermal cell counts were taken from the abaxial surface of mature, fully expanded leaves or cotyledons. Cell counts were taken from the widest section of the first true leaf avoiding the mid vein. Dental resin (Coltene Whaledent) was applied in the region of maximum leaf width and left to set before removing the leaf and applying clear nail varnish to the resin. Stomatal counts were determined from nail varnish impressions by light microscopy (Olympus BX51). Five areas per leaf were sampled from four to eight plants of each genotype and treatment. For epidermal imaging (Fig. 2B–D), mature leaves were excised and the central vein of the leaf cut away. Leaf tissue was then serially dehydrated in ethanol. Samples were then placed into modified Clarke's solution (4:1 ethanol to glacial acetic acid solution) then cleared in 50% bleach overnight.

For epidermal phenotyping, the second fully expanded mature leaf of seedlings was excised and a 3- to 5-cm strip midway along the proximodistal axis of these leaves were cut out. These leaf samples were then submerged in Clarke's solution (3:1 ethanol to glacial acetic acid solution). Following 1 h of vacuum infiltration, the samples were left in Clarke's solution for 24 h for fixation. Once fixed, the samples were transferred into 100% ethanol. Prior to imaging, the leaf samples were cleared in 50% bleach solution overnight. The midrib of each sample was then excised and the remaining leaf sections mounted in deionized water on microscope slides for imaging. Samples were viewed by light microscopy (Olympus BX51) using differential interference contrast functionality. For confocal microscopy (Figs. 4, A and B), barley samples were prepared as described (Wuyts et al., 2010) and viewed on an Olympus FV1000 using a 20× UPlan S-Apo N.A. 0.75 objective, 543-nm laser, 555- to 655-nm emission, and Fluorview software.

Physiological Measurements

Throughout the terminal drought experiment, the light-adapted ΦPSII was measured daily for both well-watered and water-withheld plants. The most recent fully expanded leaf of the primary tiller was selected for the measurement at day 1, and the same leaf was then monitored throughout the experiment. Readings were taken using a FluorPen FP100 (Photon Systems Instruments) with a saturating pulse of 3,000 μmol m^{-2} s^{-1}. Following the onset of the drought treatment, the pots were weighed every day and used to calculate the percentage of initial soil water content remaining. Well-watered controls were maintained at 60% soil water content.

Leaf RWC was determined from excised leaves from well-watered or droughted plants and their fresh weight being measured immediately, and leaves were floated on water overnight and weighed to record the hydrated weight. They were oven-dried overnight and weighed to obtain their dry weight; the RWC was calculated using the following formula: RWC (%) = (fresh weight − dry weight)/ (hydrated weight − dry weight)*100.

A LI-6400 portable photosynthesis system (Licor) was used to carry out infrared gas analysis (IRGA) on the sixth, fully expanded leaf from the primary tiller while still attached to the plant. Relative humidity inside the IRGA chamber was kept at 60% to 65% using self-indicating desiccant, flow rate was set at 300 μmol s^{-1}, and leaf temperature at 20°C. Reference [CO_2] was maintained at 500 ppm and light intensity at 200 μmol m^{-2} s^{-1}. Plants were allowed to equilibrate for 40 to 45 min the IRGA chamber being matched at least every 15 min. Once readings were stable measurements were taken every 20 s for 5 min. For soil water content calculations, the weight of pots containing water-saturated (100% water content) or oven-dried (0%) compost mix was first determined. Pots were then maintained at either 60% or 25% soil water content by weighing and addition of the appropriate amount of water every 2 d.

For carbon isotope discrimination (Fig. 6D), $\delta^{13}C$ was assessed from the flag leaf of five plants from each of the two watering regimes (well-watered and restricted-watered), as described previously (Hepworth et al., 2015).

Once plants had matured and dried down, the plants were harvested, with the total number and weight of seeds per plant being recorded and the average seed weight being calculated. All aboveground vegetative tissue was dried in an oven at 80°C for 2 d and then weighed to provide the dry weight. Harvest index (ratio of yield to aboveground biomass) was then calculated.

Statistical Analysis

All comparisons were performed on Graph Pad Prism software. The appropriate posthoc tests were conducted once significance was confirmed using an ANOVA test and an alpha level ≤0.05 or below as significant.

Accession Numbers

Sequence data from this article can be found in the GenBank/EMBL data libraries under accession numbers MF095055 and MF095056 for HvEPF1 and HvEPF2 respectively.

Supplemental Data

The following supplemental materials are available.

Supplemental Figure S1. Phylogenetic tree of predicted Arabidopsis and barley epidermal patterning factor peptide sequences constructed using Multalin.

Supplemental Figure S2. Growth of barley plants is inhibited by the water-restricted conditions used in this study.

Supplemental Figure S3. Plant heights of controls and *HvEPF1OE*-1 or *HvEPF1OE*-2 were not significantly different within either well-watered or water-restricted conditions.

Supplemental Figure S4. Aboveground biomass of control and *HvEPF1OE*-1 or *HvEPF1OE*-2 plant lines were not significantly different under either well-watered or water-restricted conditions.

Supplemental Figure S5. Schematic of the gene expression construct inserted into the barley genome to overexpress the *HvEPF1* gene.

Supplemental Figure S6. qPCR results confirming significant overexpression of *HvEPF1* the barley lines detailed in the manuscript.

Supplemental Figure S7. Plant heights of controls and HvEPF10E-1 or HvEPF10E-2 were not significantly different under either well-watered or water-restricted conditions.

Supplemental Figure S8. Aboveground biomass of control and HvEPF10E-1 or HvEPF10E-2 plant lines was not significantly different under either well-watered or water restricted conditions.

Supplemental Figure S9. Schematic of the gene expression construct inserted into the barley genome to overexpress the HvFPF1 gene.

Supplemental Figure S10. qPCR results confirming the significant overexpression of HvEPF1.

Supplemental Table S1. Copy number data for transformed plant lines used in this study.

Supplemental Table S2. Primer sequences used for PCR and RT-qPCR detailed in "Methods."

ACKNOWLEDGMENTS

We thank Dr. Jennifer Sloan for help with seed harvest and Dr. Heather Walker and Gemma Newsome for assistance with mass spectrometry.

Received February 6, 2017; accepted April 27, 2017; published May 1, 2017.

LITERATURE CITED

Adrian J, Chang J, Ballenger CE, Bargmann BO, Alassimone J, Davies KA, Lau OS, Matos JL, Hachez C, Lanctot A, et al (2015) Transcriptome dynamics of the stomatal lineage: birth, amplification, and termination of a self-renewing population. Dev Cell **33:** 107–118

Bergmann DC, Lukowitz W, Somerville CR (2004) Stomatal development and pattern controlled by a MAPKK kinase. Science **304:** 1494–1497

Caine RS, Chater CC, Kamisugi Y, Cuming AC, Beerling DJ, Gray JE, Fleming AJ (2016) An ancestral stomatal patterning module revealed in the non-vascular land plant Physcomitrella patens. Development **143:** 3306–3314

Chater CC, Caine RS, Tomek M, Wallace S, Kamisugi Y, Cuming AC, Lang D, MacAlister CA, Casson S, Bergmann DC, et al (2016) Origin and function of stomata in the moss Physcomitrella patens. Nat Plants **2:** 16179

Clough SJ, Bent AF (1998) Floral dip: a simplified method for Agrobacterium-mediated transformation of *Arabidopsis thaliana*. Plant J **16:** 735–743

Davenport DC, Fisher MA, Hagan RM (1972) Some counteractive effects of antitranspirants. Plant Physiol **49:** 722–724

Doheny-Adams T, Hunt L, Franks PJ, Beerling DJ, Gray JE (2012) Genetic manipulation of stomatal density influences stomatal size, plant growth and tolerance to restricted water supply across a growth carbon dioxide gradient. Philos Trans R Soc Lond B Biol Sci **367:** 547–555

Fita A, Rodríguez-Burruezo A, Boscaiu M, Prohens J, Vicente O (2015) Breeding and domesticating crops adapted to drought and salinity: a new paradigm for increasing food production. Front Plant Sci **6:** 978

Foley JA, Ramankutty N, Brauman KA, Cassidy ES, Gerber JS, Johnston M, Mueller ND, O'Connell C, Ray DK, West PC, et al (2011) Solutions for a cultivated planet. Nature **478:** 337–342

Franks PJ, Beerling DJ (2009) Maximum leaf conductance driven by CO_2 effects on stomatal size and density over geologic time. Proc Natl Acad Sci USA **106:** 10343–10347

Franks PJW, W Doheny-Adams T, Britton-Harper ZJ, Gray JE (2015) Increasing water-use efficiency directly through genetic manipulation of stomatal density. New Phytol **207:** 188–195

Geisler MJ, Sack FD (2002) Variable timing of developmental progression in the stomatal pathway in Arabidopsis cotyledons. New Phytol **153:** 469–476

Godfray HCJ, Beddington JR, Crute IR, Haddad L, Lawrence D, Muir JF, Pretty J, Robinson S, Thomas SM, Toulmin C (2010) Food security: the challenge of feeding 9 billion people. Science **327:** 812–818

Han S-K, Torii KU (2016) Lineage-specific stem cells, signals and asymmetries during stomatal development. Development **143:** 1259–1270

Hara K, Kajita R, Torii KU, Bergmann DC, Kakimoto T (2007) The secretory peptide gene EPF1 enforces the stomatal one-cell-spacing rule. Genes Dev **21:** 1720–1725

Hara K, Yokoo T, Kajita R, Onishi T, Yahata S, Peterson KM, Torii KU, Kakimoto T (2009) Epidermal cell density is autoregulated via a secretory peptide, EPIDERMAL PATTERNING FACTOR 2 in Arabidopsis leaves. Plant Cell Physiol **50:** 1019–1031

Harwood WA, Bartlett JG, Alves SC, Perry M, Smedley MA, Leyland N, Snape JW (2009) Barley transformation using Agrobacterium-mediated techniques. Methods Mol Biol **478:** 137–147

Hepworth C, Doheny-Adams T, Hunt L, Cameron DD, Gray JE (2015) Manipulating stomatal density enhances drought tolerance without deleterious effect on nutrient uptake. New Phytol **208:** 336–341

Hepworth C, Turner C, Landim MG, Cameron D, Gray JE (2016) Balancing water uptake and loss through the coordinated regulation of stomatal and root development. PLoS One **11:** e0156930

Hetherington AM, Woodward FI (2003) The role of stomata in sensing and driving environmental change. Nature **424:** 901–908

Hunt L, Gray JE (2009) The signaling peptide EPF2 controls asymmetric cell divisions during stomatal development. Curr Biol **19:** 864–869

International Barley Genome Sequencing Consortium (2012) A physical, genetic and functional sequence assembly of the barley genome. Nature **491:** 711–716

IPCC (2014) Climate Change 2014: Synthesis Report. Contribution of Working Groups I, II and III to the Fifth Assessment Report of the Intergovernmental Panel on Climate Change. Core Writing Team, R.K. Pachauri and L.A. Meyer, eds, IPCC, Geneva, Switzerland, 151 pp

Lau OS, Bergmann DC (2012) Stomatal development: a plant's perspective on cell polarity, cell fate transitions and intercellular communication. Development **139:** 3683–3692

Lawson S, Pijut P, Michler C (2014) The cloning and characterization of a poplar stomatal density gene. Genes Genomics **36:** 427–441

Liu T, Ohashi-Ito K, Bergmann DC (2009) Orthologs of *Arabidopsis thaliana* stomatal bHLH genes and regulation of stomatal development in grasses. Development **136:** 2265–2276

Liu Y, Yuan J, Ma H, Song J, Wang L, Weng Q (2015) Characterization and functional analysis of a B3 domain factor from *Zea mays*. J Appl Genet **56:** 427–438

MacAlister CA, Ohashi-Ito K, Bergmann DC (2007) Transcription factor control of asymmetric cell divisions that establish the stomatal lineage. Nature **445:** 537–540

Miskin E, Rasmusson DC (1970) Frequency and distribution of stomata in barley. Crop Sci **10:** 575–578

Ohashi-Ito K, Bergmann DC (2006) Arabidopsis FAMA controls the final proliferation/differentiation switch during stomatal development. Plant Cell **18:** 2493–2505

Ohki S, Takeuchi M, Mori M (2011) The NMR structure of stomagen reveals the basis of stomatal density regulation by plant peptide hormones. Nat Commun **2:** 512

Peterson KM, Rychel AL, Torii KU (2010) Out of the mouths of plants: the molecular basis of the evolution and diversity of stomatal development. Plant Cell **22:** 296–306

Pillitteri LJ, Torii KU (2007) Breaking the silence: three bHLH proteins direct cell-fate decisions during stomatal development. BioEssays **29:** 861–870

Qi X, Han SK, Dang JH, Garrick JM, Ito M, Hofstetter AK, Torii KU (2017) Autocrine regulation of stomatal differentiation potential by EPF1 and ERECTA-LIKE1 ligand-receptor signaling. eLife **6:** 6

Raissig MT, Abrash E, Bettadapur A, Vogel JP, Bergmann DC (2016) Grasses use an alternatively wired bHLH transcription factor network to establish stomatal identity. Proc Natl Acad Sci USA **113:** 8326–8331

Raissig MT, Matos JL, Gil MX, Kornfeld A, Bettadapur A, Abrash E, Allison HR, Badgley G, Vogel JP, Berry JA, et al (2017) Mobile MUTE specifies subsidiary cells to build physiologically improved grass stomata. Science **355:** 1215–1218

Ran J-H, Shen T-T, Liu W-J, Wang X-Q (2013) Evolution of the bHLH genes involved in stomatal development: implications for the expansion of developmental complexity of stomata in land plants. PLoS One **8:** e78997

Rohila JS, Chen M, Cerny R, Fromm ME (2004) Improved tandem affinity purification tag and methods for isolation of protein heterocomplexes from plants. Plant J **38:** 172–181

Serna L (2011) Stomatal development in Arabidopsis and grasses: differences and commonalities. Int J Dev Biol **55:** 5–10

Simmons AR, Bergmann DC (2016) Transcriptional control of cell fate in the stomatal lineage. Curr Opin Plant Biol **29:** 1–8

Stebbins GL, Jain SK (1960) Developmental studies of cell differentiation in the epidermis of monocotyledons: I. Allium, rhoeo, and commelina. Developmental Biology **2:** 409-426

Stebbins GL, Khush GS (1961) Variation in the organization of the stomatal complex in the leaf epidermis of monocotyledons and its bearing on their phylogeny. Am J Bot **48:** 51–59

Van Vuuren MMI, Robinson D, Fitter AH, Chasalow SD, Williamson L, Raven JA (1997) Effects of elevated atmospheric CO2 and soil water availability on root biomass, root length, and N, P and K uptake by wheat. New Phytol **135:** 455–465

Wang H, Ngwenyama N, Liu Y, Walker JC, Zhang S (2007) Stomatal development and patterning are regulated by environmentally responsive mitogen-activated protein kinases in Arabidopsis. The Plant Cell **19:** 63-73

Wuyts N, Palauqui J-C, Conejero G, Verdeil J-L, Granier C, Massonnet C (2010) High-contrast three-dimensional imaging of the Arabidopsis leaf enables the analysis of cell dimensions in the epidermis and mesophyll. Plant Methods **6:** 17

Yoo CY, Pence HE, Hasegawa PM, Mickelbart MV (2009) Regulation of transpiration to improve crop water use. Crit Rev Plant Sci **28:** 410–431

Yoo CY, Pence HE, Jin JB, Miura K, Gosney MJ, Hasegawa PM, Mickelbart MV (2010) The Arabidopsis GTL1 transcription factor regulates water use efficiency and drought tolerance by modulating stomatal density via transrepression of SDD1. Plant Cell **22:** 4128–4141

Yu H, Chen X, Hong Y-Y, Wang Y, Xu P, Ke S-D, Liu H-Y, Zhu J-K, Oliver DJ, Xiang C-B (2008) Activated expression of an Arabidopsis HD-START protein confers drought tolerance with improved root system and reduced stomatal density. Plant Cell **20:** 1134–1151

Zhao L, Sack FD (1999) Ultrastructure of stomatal development in Arabidopsis (Brassicaceae) leaves. Am J Bot **86:** 929–939